

V-I Characteristics of Ag_2S -Element at Low Temperature

Saburo Muto

Department of Electrical Engineering

(Received September 9, 1976)

The author has clarified the nonlinearity of the V-I (voltage vs. current) characteristics of Ag_2S powder compressed into a disc shape (14.5 mm ϕ , 5 mm thickness), when a pair of brass electrode are attached to the both sides of the disc element and AC voltage of 60 Hz is applied. It is shown that the element can be used as a switching element in the electric power applications such as electric power fuses.

The authors also succeeded in deriving a theoretical equation for the nonlinear V-I characteristics by assuming the phase transition phenomenon of Ag_2S from β -to α -phase takes place in the channel-like conducting part formed in the element.

The theoretical equation agreed very satisfactory with the actual measured values at the element surrounding temperature of near room temperature. In this paper the agreement between the theoretical equation and a set of measured values is examined for different surrounding temperature from the cryogenic temperature attained by liquid nitrogen to phase transition temperature of Ag_2S (179°C).

It is concluded that the derived equation shows satisfactory agreement with the measured values within the error range of physical constants.

INTRODUCTION

Under the phase transition temperature 179°C from β -to α -phase Ag_2S has resistance with a negative temperature coefficient peculiar to semiconductors, which is about $1 \times 10^{-1}/^\circ\text{C}$ for room temperature.

The resistance decreases by three digits at the transition point, above which α - Ag_2S has very small resistivity of about $10^{-3} \Omega \cdot \text{cm}$ and shows metallic conductivity with a slight positive temperature coefficient.

The author has published a paper "Non linear Characteristics of Ag_2S Element used in some Power Device", which is contained to this paper to investigate the agreement between the theoretical equation proposed by the authors and actual experimental values at the element surrounding temperature ranging from the nitrogen cryogenic temperature to 179°C, assuming the internal formation of conducting channel.

Ag_2S is a sort of amorphous semiconductor with

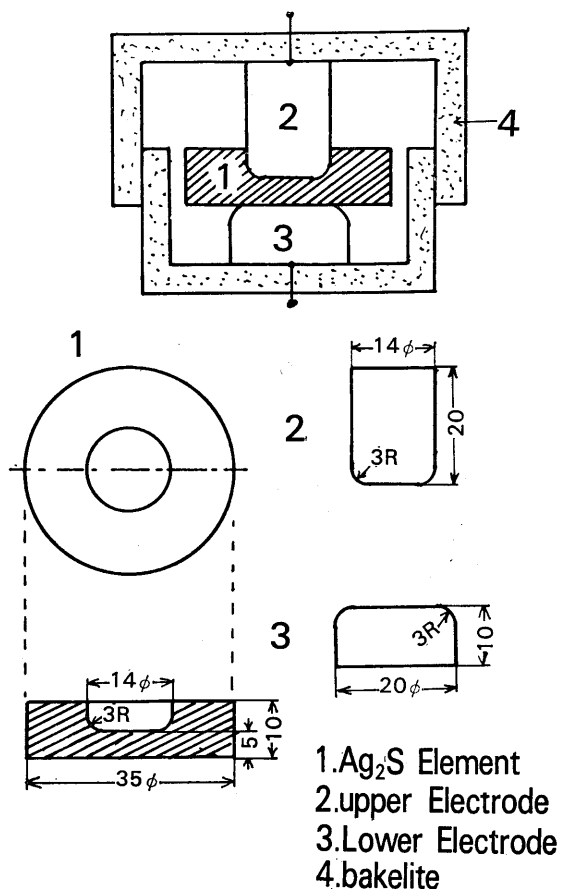
the physical constants as shown in Table I, so that the physical clarification of the V-I characteristics and its mechanism is very important from the viewpoints of switching characteristics of amorphous semiconductors. This study also aims at development of new potential application of Ag_2S to protective elements for the low-temperature cable systems.

EXPERIMENTAL EQUIPMENTS AND METHOD OF MEASUREMENT

Powder of Ag_2S is compressed to shape a disc type of diameter 35mm, which is inserted between a upper and lower brass electrode of 14mm and 20mm diameter respectively. The gap length as shown in Fig. 1 is held at 5mm in order to eliminate the surface flashover phenomena. The element is maintained at low temperature as shown in Fig. 2. Fig. 2-A shows the configuration of the equipment to maintain the low temperature between 0°C and the temperature of dry ice and Fig. 2-B shows the equipment for the

Table I Physical Constants of Ag_2S

Molec. form.	Ag_2S
Molec. Weight	$M=247.83$
State at room-temp.	grayish black colored powder
transit. temp.	$T_c=180^\circ\text{C}$ (179°C 175°C) higher temp. from T_c : α phase
melt. temp.	$T_m=845^\circ\text{C}$ (825°C 838°C)
Molec. heat C_p Specific heat C $C=C_p/M$ [cal·g ⁻¹ ·°C ⁻¹]	$-180^\circ\text{C}\sim 15^\circ\text{C}$: $C_p=14.08$, $C=0.0568$ $15^\circ\text{C}\sim 100^\circ\text{C}$: $C_p=18.26$, $C=0.0737$ $15^\circ\text{C}\sim 324^\circ\text{C}$: $C_p=22.38$, $C=0.0903$ 20°C : $C_p=17.87$, $C=0.0722$ $15^\circ\text{C}\sim 100^\circ\text{C}$: $C_p=19.92$, $C=0.0804$
density [g·cm ⁻³]	nature argentite: 7.26~7.31 acanthite: 7.31~7.36 artificially: 6.80~7.00 :7.32, 7.317 :7.326
α phase	$a=4.88\text{\AA}$ (at 250°C)
β phase	$a_0=4.32\text{\AA}$ $b_0=6.93\text{\AA}$ $c_0=7.86\text{\AA}$ $B=99.61^\circ$
heat conductivity	$k=1.2\times 10^{-3}$ [cal·°C ⁻¹ ·cm ⁻¹ ·sec ⁻¹] at β phase
resistivity g	α phase: 10^{-3} [Ω ·cm] β phase: $g=10^{4.279}\times \exp(-0.0563T)$ [Ω ·cm] $\langle T: ^\circ\text{C} \rangle$ α phase: about 10^{-3} [Ω ·cm] β phase: $g=10^{3.300}\times \exp(-0.0395T)$ [Ω ·cm] $\langle T: ^\circ\text{C} \rangle$

Fig. 1 Element of Ag_2S and electrode of brass

cryogenic temperature range using liquid nitrogen.

Extreme attention is paid to the measurement of V-I characteristics in order to eliminate the leakage current paths, since the V-I characteristics should be

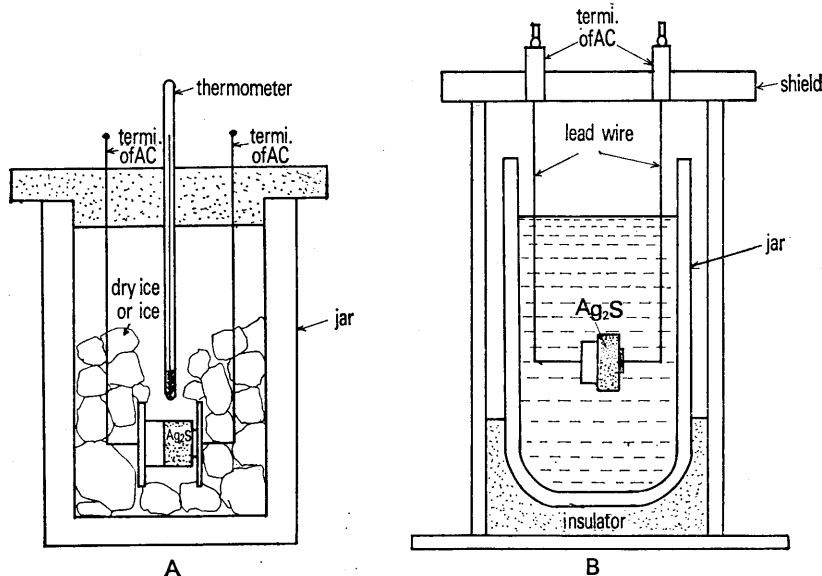


Fig. 2 The configuration of the experiment A; The equipment for the low temperature between 0°C and the temperature of dry ice B; The equipment for the cryogenic temperature

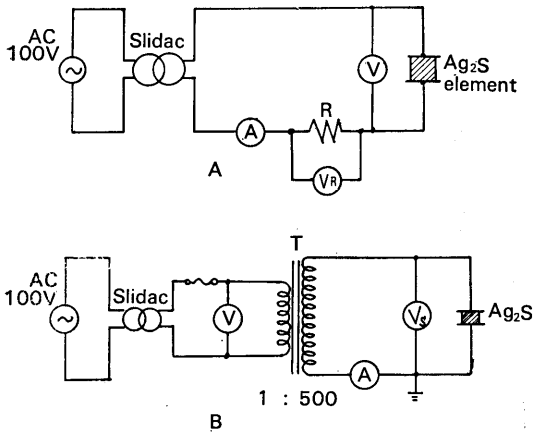


Fig. 3 Experimental circuits A; Circuit for the room temperature and the low temperature, B; Circuit for the cryogenic temperature

determined by the internal current of the element. It is necessary to apply AC voltage of several times of 10KV to the element at the cryogenic temperature ranges, so that a special measuring circuit shown in Fig 3-B is used in this case. The circuit shown in Fig. 3-A is sufficient in the other cases, since the applied voltage is low. Static voltmeter is used to measure the applied voltage.

V-I CHARACTERISTICS OF ELEMENT

The curves A and B in Fig. 4 shows the V-I characteristics of Ag_2S element shown in Fig. 1 at room temperature $16^\circ C$ using the circuit of Fig. 3-A. The characteristic curves vary with different shapes of the elements. The curves A and B correspond to the disc shaped Ag_2S elements of the diameter 14mm and thickness 5 mm and that of Fig. 1 respectively.

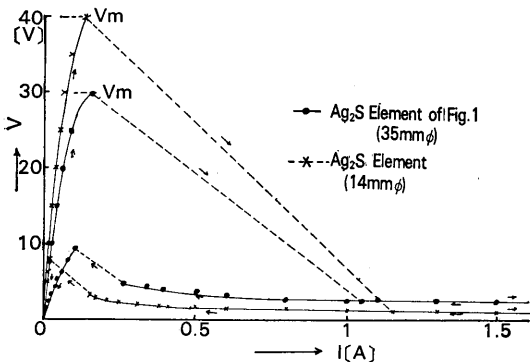


Fig. 4 The V-I characteristics of Ag_2S element shown in Fig. 1

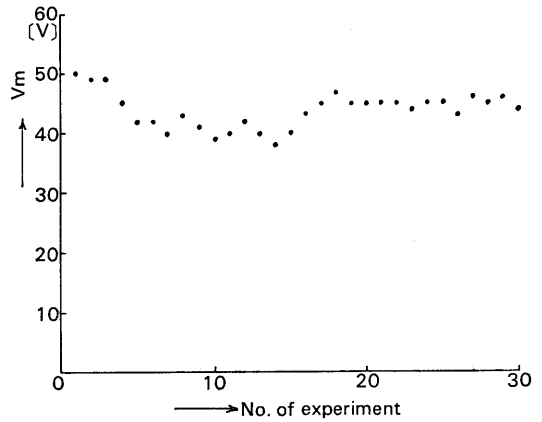


Fig. 5 The distribution of the transition voltage V_m

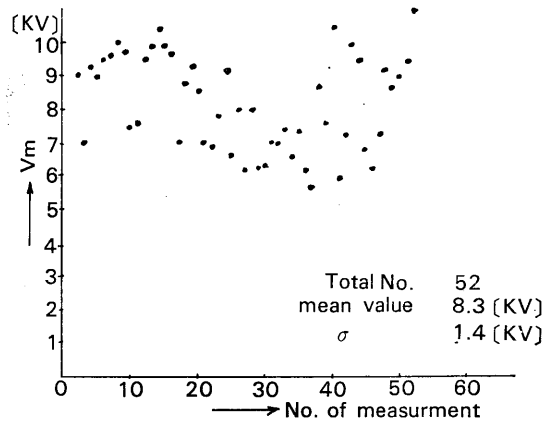


Fig. 6 A set of scattering value of V_m to number of measurements

Both curves show the typical switching characteristics. It is also known that Ag_2S elements have a property in taking different trajectories for increasing and decreasing voltage.

The measuring are carried about 30 times using many elements and the relationship between the measuring number and the transition voltage V_m is plotted in Fig. 5 to show the distribution within a certain range of fluctuation.

The outcomes of the experiments are then expressed by a histogram as Fig. 7-A. The distribution of V_m can be approximated by a normal distribution with the mean value $V_{m0}=43.75 [V]$.

Secondly, the element of Fig. 1 is immersed in liquid nitrogen as shown Fig 2-B and kept in Dewar to measure V-I characteristics. It is observed, in this

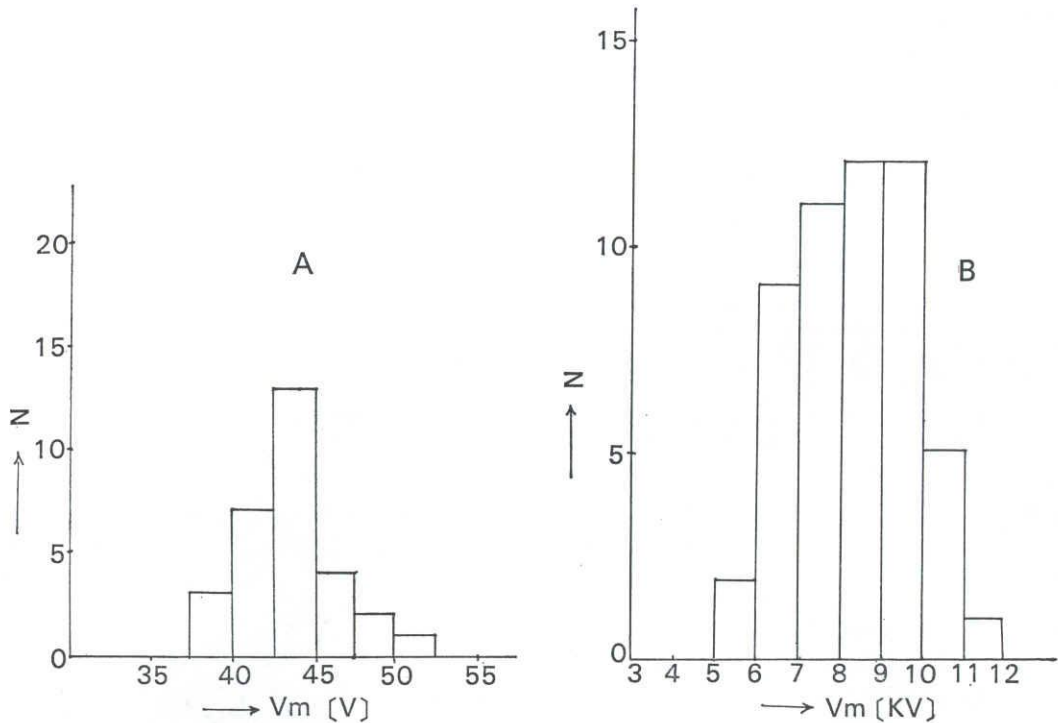


Fig. 7 The histogram of V_m
 A; Experimental results of Fig. 5
 B; Experimental results of Fig. 6

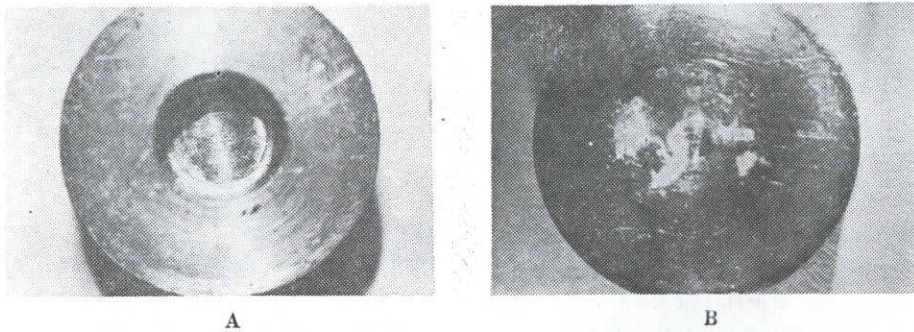


Fig. 8 The photograph of the current trace on the surfaces of Ag_2S element
 A; Upper side of the Ag_2S element shown Fig. 1
 B; Down side of the same element

case, that the phase transition voltage is very high and climbs up to 200 times of V_m at room temperature.

The number of measurements in this case is 52 and the number and V_m are plotted in Fig. 6, which shows a set of scattering values of V_m . The relationship between V_m and the measurement number are expressed in the form of a histogram as Fig. 7-B. The distribution can be approximated by a normal distribution with a mean value $V_{m0}=8.3$ [KV] and a standard deviation $\sigma=1.4$ [KV].

In order to confirm the location of the current paths in the Ag_2S elements and the upper and lower electrode are taken out from liquid nitrogen to the atmosphere and the traces on the surfaces formed by the passing current are shown by the pictures, Fig. 8-A, -B and Fig. 9-A, -B.

Fig. 8-A shows the trace developed on the surface of the Ag_2S element of Fig. 1 after an experiment and a trace of the current path caused by the phase transition is found in the follow.

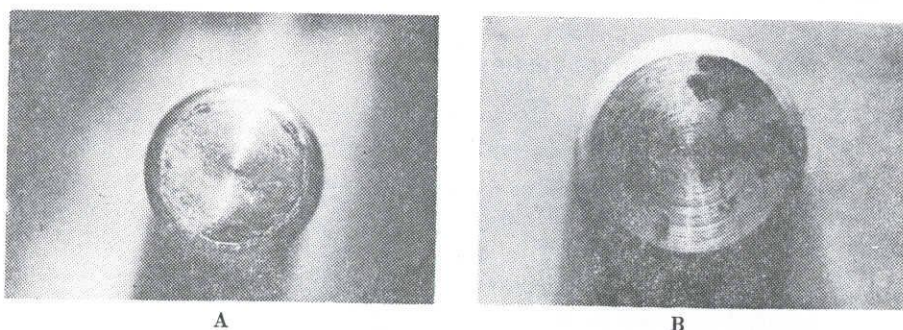


Fig. 9 The photograph of the current trace on the surfaces of brass electrode
A; Traces of the current of the upper electrode of Fig. 1
B; Traces of the current of the lower electrode of Fig. 1

Fig. 8-B shows a trace on the backside of the same element and a discolored current trace distribution around the central part is recognized.

Fig. 9-A shows the lower side of the upper electrode with discolored circle on the edge of the electrode showing the current trace. Fig. 9-B shows the current trace on the surface of the lower electrode attached to the element and a number of concentrated current traces are recognized on the right upper part of the electrode.

These pictures of resulting trace justify the author's theory that the current paths are assumed to be formed in the internal part of the Ag_2S elements and the path do not go through the elements uniformly but through a certain channel-shaped conducting path.

DERIVATION OF THEORETICAL EQUATION

As discussed in detail in the reference [1], Wager's theory, which is well known as a thermal breakdown theory in the solid insulator is applied to the internal current conduction property of Ag_2S .

It is assumed that there is a path in the element placed between the upper and lower electrode from the every beginning and the path has higher conductivity for uneven local current. With this assumption, it may be well estimated that the path has higher temperature increasing speed compared to the other part and thus forms a channel-like conductive path by the high temperature and high current density.

Neglecting the thermal diffusion to the direction of the axis (z axis) of the channel part, Eq. (1) is obtained by considering the thermal diffusion to the radius direction.

$$\kappa \frac{\partial^2 T}{\partial r^2} + \kappa \frac{1}{r} \frac{\partial T}{\partial r} + 0.24 \sigma_0 e^{\alpha T} \frac{V^2}{j^2} = c \rho \frac{\partial T}{\partial t} \quad (1)$$

Table II Definition of Symbols

Symbols	Definitions
T	Temperature in an Ag_2S element
r	Distance from the center of an Ag_2S element
K	Heat conductivity
P	Irregularity factor of electric conductivity
$\sigma_0 e^{\alpha T}$	Electric conductivity at $T^\circ\text{C}$
l	Thickness of an Ag_2S element
V	Impressed Voltage (rms of AC)
C	Specific heat
ρ	Density of Ag_2S
T_c	room temperature

Table II shows the definition of symbols of the equation (1). Although Eq. (1) is a general equation, it is assumed here that the all injected Joule's heat into the element is approximately consumed only by the temperature rise in the channel part.

In this case, only the third term in Eq.(1) remains and the time application of voltage V is given by eq. (2).

$$t_0 = \frac{c \rho l^2 e^{-\alpha T_c}}{0.24 P \sigma_0 V^2 \alpha} \quad (2)$$

In Eq. (2), by substituting $C=0.06$, $\rho=7.3$, $l=0.5$, $\alpha=0.056$, and $\sigma_0=10^{-4.3}$, the relationship between V and the surrounding temperature T_c can be obtained for given to.

For example, let the phase transition time $t_0=5$ [s]. In this case,

$$\log_{10} V = 2.26 - 0.012 T_c \quad (3)$$

If $t_0=20$ [s],

$$\log_{10} V = 1.96 - 0.012 T_c \quad (4)$$

As is shown, there is a linear relationship between $\log_{10} V$ and T_c .

COMPARISON OF EXPERIMENT WITH THEORY

As described in chapter 3, a set of experiments is carried out for different surrounding temperature of a wide range such as $T_c=16^\circ\text{C}$ (room temperature), $T_c=179^\circ\text{C}$ (phase transition temperature) and $T_c=196^\circ\text{C}$ (liquid nitrogen), and each measured V_m of V-I characteristics is plotted with $\log V_m$ as ordinate against T_c as abscissa. In almost linear relation shown by the line A in Fig. 10 is obtained.

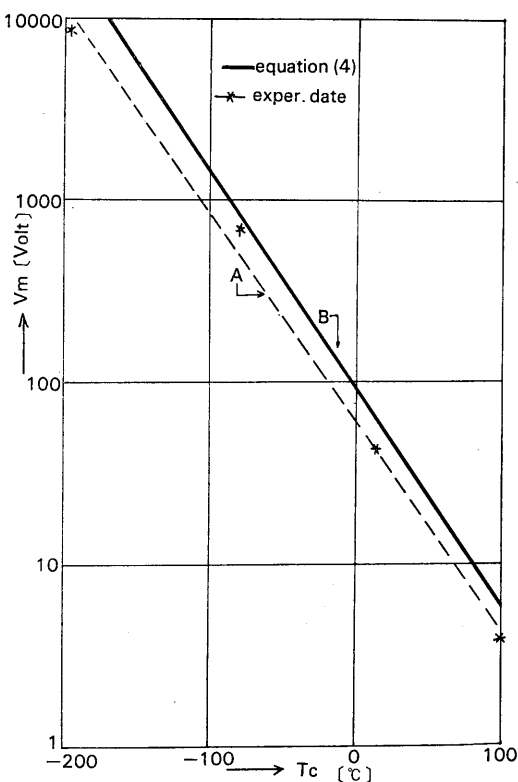


Fig. 10 Theoretical results and experimental data of the characteristics line of $\log V_m - T_c$.

The line B in Fig. 10 is attained by plotting Eq. (4). The line obtained by the experiments does not agree with the line B by theoretical calculation completely.

If the theoretical equation, however, takes the form as expressed by the following equation (5) instead of Eq. (4), both lines can agree completely with each other.

$$\log_{10} V = 1.88 - 0.011 T_c \quad (5)$$

If Eq. (4) is modified to coincide with the theo-

retical Eq. (5), a set of constants substituted into Eq. (2) to yield Eq. (4) have to be changed much or less.

After calculation, the constants used in Eq. (4) listed in the second column of Table III are modified to those in the third column in order to obtain agreement with Eq. (5).

Table III Comparison between theoretical and experimental values

Symbols[unit]	theoretical value from equation (4)	experimental value equation (5)
α $1/^\circ\text{C}$	0.056	0.050
σ_0 $\Omega^{-1}\text{cm}^{-1}$	$10^{-4.3}$	$10^{-3.5} \sim 10^{-4.1}$
t_0 sec	20	5 ~ 20

DISCUSSION

According to Fig. 10, it is observed that the difference between the line A and B is approximately negligible and on the other hand, the theoretical voltage is higher than the experimental voltage V_m at the cryogenic temperature.

The disagreement of this amount, however, can be attributed to the slight difference in the physical constants, (α , σ_0 , etc.) of Ag_2S as shown in Table III.

It is quite reasonable to conclude that the variation in the physical constants is within an acceptable region, since the Ag_2S material is different from a lot to the other and it is concluded that the theoretical equation of the characteristics derived by the author's agrees with the actual measured values.

ACKNOWLEDGEMENT

The author wishes to express their indebtedness to Messrs. K. Inoue, T. Murakoshi and H. Watanabe for their assistance in this study as a partial fulfillment of their undergraduate course work. And thanks also to Messrs. K. Nakamura and H. Kobayashi, assistant of N.I.T.

REFERENCES

- (1) P. Junod; *Helv. Phys. Acta.* **32**, 567 (1959)
- (2) R. G. Cope & H.J. Coldmid; *Brit. J. App. Phys.*, **16**, 1501 (1965)
- (3) S. Muto, Y. Watanabe & T. Kajita; *J.I.E.E. of Japan*, **89**, 2378 (1969)